Geological Society of America
Special Paper 180
1979

A model of pyroclastic surge

K. H. Wohletz
University of California, Los Alamos Scientific Laboratory, Los Alamos, New Mexico 87545

M. F. Sheridan
Department of Geology, Arizona State University, Tempe, Arizona 85281

ABSTRACT

Pyroclastic-surge deposits vary in size from those associated with large ash-flow sheets surrounding calderas to tuff rings formed during small phreatomagmatic explosions. This paper results from studies of pyroclastic-surge deposits at Crater Elegante, Sonora, Mexico; Peridot Mesa, Arizona; Coronado Mesa, Arizona; Ubehebe Crater, California; and the Bishop Tuff, California. Stratigraphic sections measured at varying distances from the vents are input for a Markov analysis of bed-form transitions, through which facies of pyroclastic surge are defined.

The principal bed forms are massive beds, planar beds showing inverse grading, and sandwave beds with dunes, ripple and cross laminations, and antidunes. Markov analysis shows that sections are characterized by a dominance of either (1) sandwave and massive beds (sandwave facies); (2) planar, massive, and sandwave beds (massive facies); or (3) planar and massive beds (planar facies). Facies distribution maps demonstrate a systematic lateral variation away from the vent. Sandwave facies predominate in sections nearest the vent, massive facies dominate in sections at an intermediate distance from the vent, and planar facies occur in sections farthest from the vent.

The spatial distribution of surge facies is compatible with a fluidization-deflation model of pyroclastic-surge transport and deposition. A pyroclastic-surge cloud that is initially fluidized at the vent deflates (defluidizes) as it moves laterally. During transport the cloud passes from a proximal viscous mode of flow characterized by deposition of the sandwave facies to a distal inertial mode of flow represented by deposition of the planar facies. The gradual transition from viscous to inertial flow is coincident with deposition of the massive facies.

INTRODUCTION

The term "pyroclastic surge" was first suggested by Sparks (1976) as a synonym for "ground surge" (Sparks and others, 1973) so that pyroclastic deposits could be placed into a tripartite classification: pyroclastic fall, pyroclastic flow, and pyroclastic surge. The concept of pyroclastic surge is an offshoot from that of base surge. The base surge is a ring-shaped cloud that moves horizontally outward at hurricane velocities as a turbulent density current from the base of a vertical explosion column. The explosion may be due to underground or underwater nuclear or chemical detonation, volcanic eruption, or possibly hypervelocity impact upon a planetary body. Numerous workers have described base surge related to nuclear events, and Richards (1959) and Moore (1967) were among the first to apply the concept to volcanic eruptions. Fisher (1966) mentioned base surge as a possible dispersal mechanism of ash flows, and in following years, Fisher and other workers documented base surge and its deposits associated with volcanic eruptions of a phreatomagmatic type.

As a result of photogeologic mapping of the lunar surface, the existence of patterned ground in impact ejecta blankets (especially around multiringed basins) led to the speculation that a surgelike dispersal mechanism may accompany impact events (Masursky, 1968; Fisher and Waters, 1969). Later experimental investigations (Gault, 1973) and theoretical developments of impact mechanisms questioned the idea of impact-related base surge. Despite these results, detailed study of the Martian and lunar surfaces in light of the facies model presented here, as well as a realization of the complexity of impact events, makes surge an attractive mechanism for modification of planetary landscape by impact.

Because the term "base surge" has been applied to terrestrial and nonterrestrial events of widely varying mechanisms, its definition has become so broad as to make it less meaningful. For this reason, the term "pyroclastic surge" is recommended as a more appropriate term for volcanic events. Pyroclastic surge may be distinguished from pyroclastic flow in that surge refers to a time-transient, unsteady flow of tephra that occurs as a pulse or series of pulses in which the kinetic energy rapidly decays. Pyroclastic flow (ash flow, nuée ardente) denotes a steady stream or flood of tephra, which is able to maintain its kinetic energy over a longer time interval.

The deposits resulting from pyroclastic surges are typified by thin, continuous beds of tephra showing low-angle cross stratification, planar, and massive features as opposed to pyroclastic-flow deposits that are thickly bedded, massive, and generally nonstratified. However, Fisher (1966, 1976), Walker (1971), and Sheridan (1976) described cross and planar stratification as minor features also associated with pyroclastic flows. It is likely that surge and flow are intimately related phenomena, as borne out by field relationships described in this paper as well as by Sparks and others (1973) and Walker (1971).

Since the first recognition of pyroclastic surge as an important emplacement process, numerous occurrences have been found. However, there are still many problems related to understanding the origin, transport, and depositional mechanism of the resulting deposit. A consensus of previous work supports the likelihood that surges are fluidized, turbulent density flows. Deposition of bed forms characteristic of a subaqueous environment (plane beds, dunes, and antidunes) has led Fisher and Waters (1970) and Crowe and Fisher (1973) to suggest that deposition occurs in the upper flow regime (Simons and Richardson, 1966) in a manner similar to deposition from debris-laden streams or turbidity currents. Accordingly, velocity of transport is a dominating factor upon deposition. More recently, Sheridan and Updike (1975) used factor analysis of the discrete grain-size populations of specific bed forms to suggest that deposition depends upon the relative influence of viscous and inertial forces during transport, by analogy with experimental results from wind tunnels and flumes (Bagnold, 1954; Sanders, 1965; Carter, 1975). According to this concept, void space within the surging cloud is the critical factor in bed-form development (Wohletz and Sheridan, 1976).

Terminology

The terminology for surge deposits and flow mechanisms partly follows that of Sheridan and Updike (1975) and Sheridan and Ragan (1976). A *fluidized system* should be defined in a more restrictive sense than used in the above papers. Our definition is "a mixture of particles (solid or liquid) suspended by an upward escaping fluid phase (liquid or gas) so that the frictional force between the fluid and the particles counterbalances the weight of the particles and the whole mass behaves as a fluid." This is contrasted with a *deflating system* which is "a mixture of particles and a fluid phase that behaves as a fluid due to the net downward displacement of particles through the fluid." Other terms related to fluidization are from Leva (1959) and Kunii and Levenspiel (1969).

Objectives and Methods of Study

Because bed forms are related to depositional environments, systematic differences over time or distance indicate changes in the transport mechanism. This study documents the character of surge deposits as a function of distance from the vent. Stratigraphic sections measured around volcanic vents illustrate systematic variations in bed forms, bed and bedding-set thicknesses, impact sags, soft-sediment deformation, and grain-size distributions that characterize surge deposits.

Some complexities make characterization of stratigraphic sections difficult: (1) temporal superposition of deposits from surges of different sizes and energies that result from the pulsating nature of surge-producing volcanic events and (2) transition from one bed form to another over centimetre intervals, making judgment of dominant bed form or bed-form ratios difficult. To overcome these problems, a statistical method is needed to characterize sections and analyze bed-form distributions. Markov analysis (Davis, 1973; Harbaugh and Bonham-Carter, 1970) was selected because it is directed toward understanding sequenced events. A sequence of events, such as the deposition of a series of beds in a stratigraphic section, displays a Markov character when the occurrence of one event (the deposition of a given bed form) is dependent in a probabilistic manner upon the preceding event.

The Markov analysis used in this study records ascending bed-form transitions within small intervals throughout stratigraphic sections. The interval (10 cm) was chosen to reflect all transitions without overweighing thicker lithologies. This interval is slightly less than the minimum average thickness of the three bedding-set types. The transitions are recorded in a square matrix in which the number of elements is the square of the number of bed types or forms recognized. Each element corresponds to a specific transition type: sandwave-sandwave (S-S), sandwave-massive (S-M), and so on. The transition matrix is usually written so that each element is the probability of the corresponding transition type. For this study three basic bed forms [sandwaves (S), massive (M), and planar beds (P)] were recognized, resulting in the three by three matrix below.

$$\begin{bmatrix} \text{S-S} & \text{S-M} & \text{S-P} \\ \text{M-S} & \text{M-M} & \text{M-P} \\ \text{P-S} & \text{P-M} & \text{P-P} \end{bmatrix}$$

The use of matrices facilitates stratigraphic analysis in several ways: (1) Matrices can be tested for the Markov property by a chi-square test in which the null hypothesis states that transitions are random (Davis, 1973); (2) matrices allow numerical characterization of a stratigraphic section; (3) matrices provide statistical means to simplify the complexities in field characterization of surge deposits; and (4) matrices are convenient for data storage, retrieval, and subsequent analysis by computer.

TABLE 1. CRATER SIZE VERSUS SPREAD OF SURGE DEPOSIT

Deposit	Diameter of structural rim (km)	Maximum distance from structural rim (km)
Coronado Mesa	0.5	1.1
Peridot Mesa	0.55	1.25
Ubehebe Crater	0.80	0.82
Sugarloaf Mountain	1.0	1.2
Elegante Crater	1.6	>1.1
Bishop Tuff	16 × 29	>15

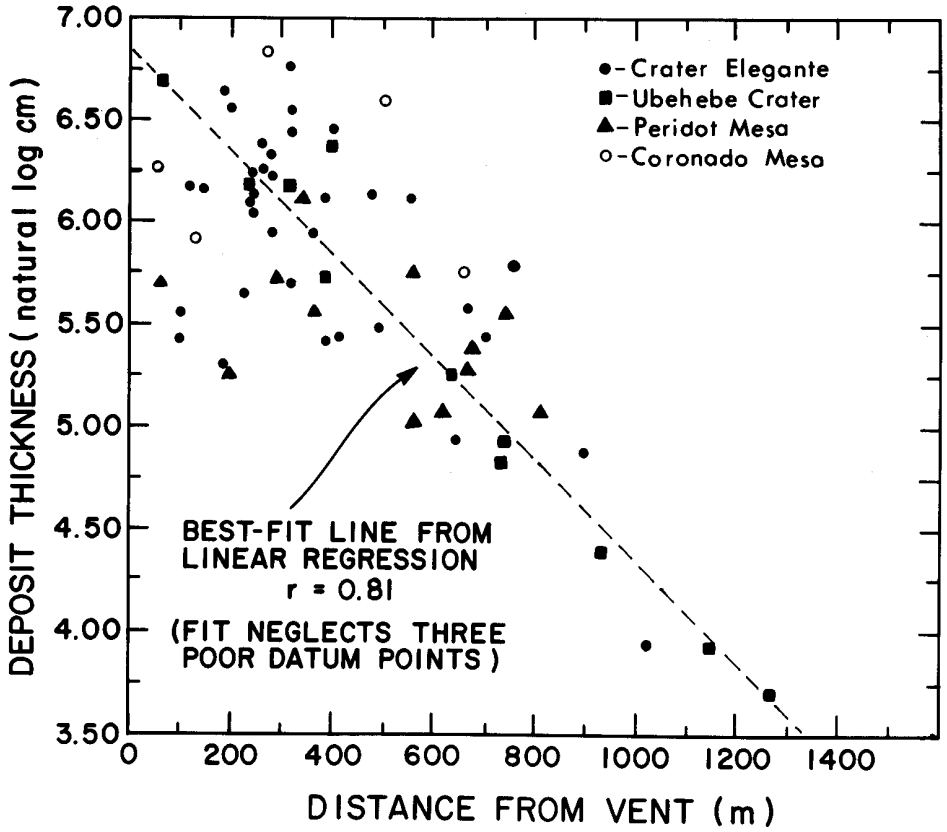

Figure 1. Plot of deposit thickness versus distance from the vent.

DEPOSITS

The surge deposits studied form an apron of poorly sorted tephra around a central vent. The maximum radial distance attained by the deposits is nearly the same as the diameter of the structural rim of the vent (Table 1). The deposits have an overall wedge shape in cross section with a nearly logarithmic decrease in thickness away from a vent (Fig. 1).

Pyroclastic-surge deposits are composed of an extremely wide range of juvenile, accessory, and accidental components. Some deposits are composed of dominantly juvenile fragments; others may consist of 90% accessory and accidental clasts. A compilation of grain-size analyses of pyroclastic-surge deposits (Table 2) shows that there are three subpopulations of sizes that correspond to the three principal bedding structures: (1) sandwave beds, (2) massive beds, and (3) planar beds. Grain-size data from Crater Elegante support the argument of Sheridan and Updike (1975) that the three subpopulations fall into discrete fields on a ternary-size diagram (Fig. 2). By Q-mode factor analysis, Sheridan and Updike (1975) found that two principal factors could account for more than 90% of the cumulative variance of grain-size data. One factor loading is associated with sandwave beds; the other factor loading is related to planar beds. Massive beds are characterized by nearly equal loadings for both factors. These factors were assigned to viscous and inertial modes of transport based on grain-size and bed-form characteristics.

Bed Forms

Sandwave Beds. Of the three principal bedding structures in pyroclastic-surge deposits, sandwaves have attracted the greatest attention of previous workers, for example, Crowe and Fisher (1973). The term "sandwave," defined as a bed form showing an undulating surface or surfaces inclined to the depositional substrate, includes bed forms such as dunes, antidunes, ripples, and cross laminations (Fig. 3). Most of these features are the result of a viscous mode of transport (Carter, 1975; Sanders, 1965), although some types of cross laminations result from an inertial (laminar, grain flow) mode of transport in a traction carpet (Sanders, 1965). Sandwave beds account for an average of 34% of all measured sections at the locations studied. The sandwave proportion of a section (Fig. 4) and the average sandwave bedding set thickness (Fig. 5) decrease approximately logarithmically with increasing distance from the vent. The average wave length also decreases with distance (Fig. 6) in agreement with previous studies (Moore, 1967; Waters and Fisher, 1971).

Planar Beds. These beds are inversely graded, which indicates that their origin was from flow as opposed to fall (which generally produces normal grading). Planar beds may be cross stratified and show internal pinch and swell features that result in a sandwave appearance. These bed forms are analogous to inversely graded beds from subaqueous density currents described by Sanders (1965), which are thought to be transported

TABLE 2. GRAIN-SIZE ANALYSIS OF PYROCLASTIC-SURGE DEPOSITS

Worker and bedform	Number of analyses	Median diameter (ϕ)*	Sorting coefficient (σ_ϕ)†
Rhyolitic surge			
Sheridan (1971)			
Sandwave beds	10	3.52 ± 0.40	2.33 ± 0.2
Plane beds	15	−0.68 ± 0.78	2.02 ± 0.28
Sheridan and Updike (1975)			
Sandwave beds	31	3.0 ± 0.8	1.9 ± 0.5
Plane beds	24	−0.5 ± 0.4	1.9 ± 0.3
Massive beds	5	1.0 ± 0.3	1.6 ± 0.3
Basaltic surge			
Fisher and Waters (1970)			
Sandwave beds	8	2.6 ± 1.0	1.4 ± 0.3
Waters and Fisher (1971)			
Sandwave beds	3	1.67 ± 0.34	0.86 ± 0.01
Plane beds	1	0.40	1.61
Crowe and Fisher (1973)			
Sandwave beds	17	1.58 ± 0.56	1.37 ± 0.18
Plane beds	5	0.19 ± 0.93	1.65 ± 0.15
Weighted mean sandwave beds		2.62 ± 0.70	1.73 ± 0.38
Weighted mean plane beds		−0.48 ± 0.28	1.88 ± 0.25
Weighted mean massive beds		1.0 ± 0.3	1.6 ± 0.3

*The phi grain size is defined as $\phi = -\log_2$ (size in mm).
†Inman (1952).

as a dense traction carpet by a laminar grain-flow mechanism. This bed form accounts for an average of 21% of all measured sections. The fraction of planar beds increases in an approximately logarithmic manner away from the vent (Fig. 7), although this plot does not properly represent those sections near the vent that contain no planar beds.

Massive Beds. They are commonly lens-shaped and exist on the lee side of dunes. Superficially they resemble small ash-flow tuffs and are mostly unstratified, ungraded, and rarely show internal structures. Massive beds may show pebble trains or stringers which give a crude internal stratification that is planar or wavelike. Massive beds are thought to be transitional between sandwave and planar beds. They may be transported by a deflating dense-phase fluidized surge and make up 45% of all measured sections. Unlike both sandwaves and planar beds, their proportion within a section does not seem to depend on distance (Fig. 8).

Other minor bedding structures are bedding sags, contorted stratification, and channels described by Crowe and Fisher (1973) and Fisher and Waters (1969).

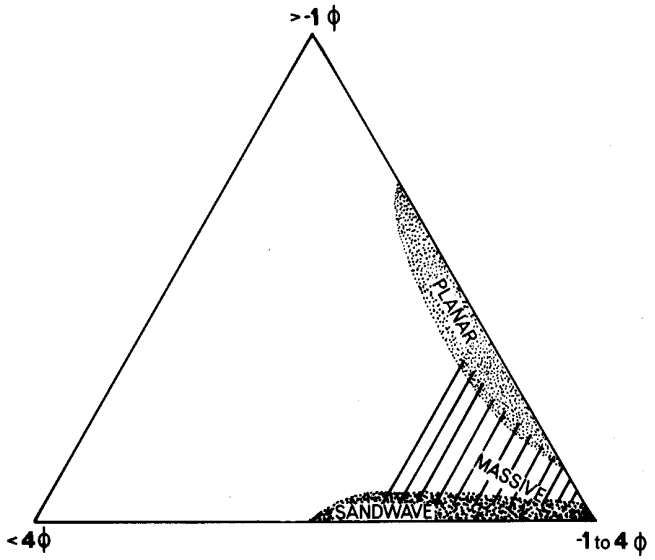

Figure 2. Grain-size fields of bed-form types. Data from Sugarloaf Mountain, Arizona (Sheridan and Updike, 1975), Crater Elegante, Surtsey, and Taal (Sheridan and Maisano, 1975).

Locations

Although pyroclastic-surge deposits are generally the result of phreatomagmatic eruptions of basaltic to rhyolitic compositions producing maarlike features, surge deposits also underlie some ash-flow sheets [the "ground surge" of Sparks and Walker, (1973)], a relationship suggested by Fisher (1966) and Walker (1971). The study localities of this paper (Fig. 9) are from a variety of volcanic settings: Crater Elegante, Northern Sonora, Mexico; Peridot Mesa, Arizona; Coronado Mesa, Arizona; Ubehebe Crater, California; and the Bishop Tuff, California.

Crater Elegante. One of eight recognized basaltic maarlike volcanoes in the Pinacate volcanic field (Jahns, 1959), this Holocene crater is 1.6 km wide and 0.24 km deep and shows evidence of an explosive collapse origin (Gutmann, 1976). Surge beds were deposited on still-fluid lava on the northwest rim of the crater. Tephra of surge origin surrounding the crater is approximately 50 m thick at the crater rim and extends out radially for slightly more than 1,100 m, although originally it extended farther.

Thirty-three stratigraphic sections were measured on the south side of the crater where exposures in gullies are excellent. Near the crater rim, bed forms are dominantly sandwave and massive. Distal parts of the deposit lack sandwave beds, and planar beds are dominant.

Peridot Mesa. This basalt flow, near San Carlos, Arizona, caps Pliocene pyroclastic surge, grus, and lake beds. The flow extruded from a diatreme that is partially encircled by a tuff ring forming a breached crater approximately 550 m in diameter. The surge deposits appear to have resulted from the more explosive, vent-clearing initial phases or eruption before extrusion of the basalt. Palagonite, accretionary lapilli, and lake-bed material in the surge tephra indicate that the surge eruption was phreatomagmatic. The surge deposit is 10 m thick adjacent

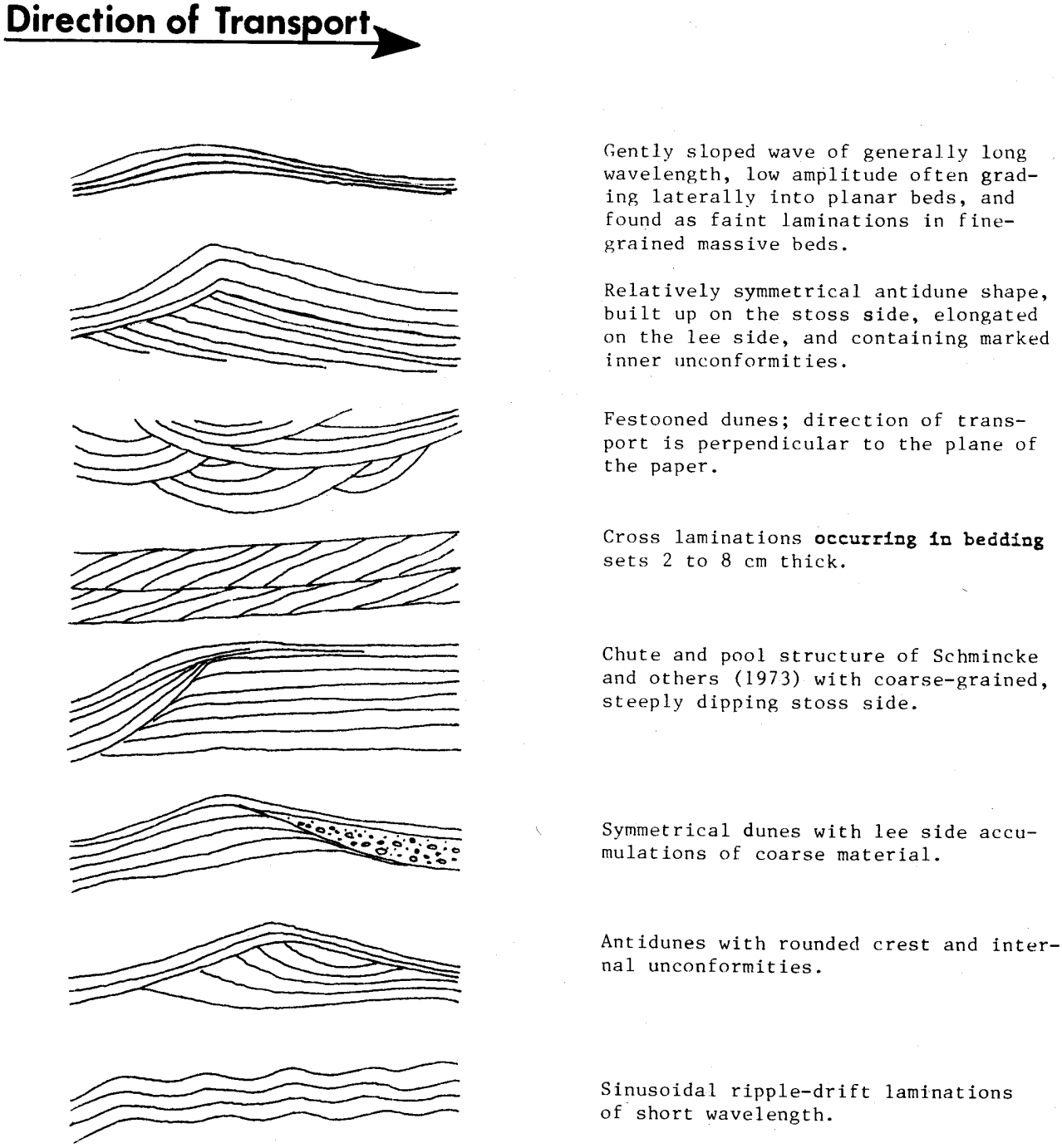

Figure 3. Morphologies of sandwaves viewed in cross section. Variation of these types occur commonly in deposits of pyroclastic surge.

to the vent where sandwave and massive bed forms are ubiquitous, but at 1,250 m from the vent, planar bed forms dominate. Dissection of the lava-capped mesa has produced excellent exposures along which 11 sections were measured.

Coronado Mesa. Located in the eastern portion of the Superstition volcanic field of Arizona (Sheridan, 1968), Corodado Mesa is near a series of ring faults that extend along Fish Creek and possibly delineate a volcano-tectonic depression or caldera northeast of the Superstition caldera (Suneson and Sheridan, 1975). Coronado Mesa is underlain by a 16.1-m.y.-old rhyolite lava flow of the Geronimo Head Formation (Stuckless and Sheridan, 1971). The lava flow caps a previously undescribed tuff ring of surge beds that is only poorly exposed.

Bedding attitude, thickness, and distribution of bed forms

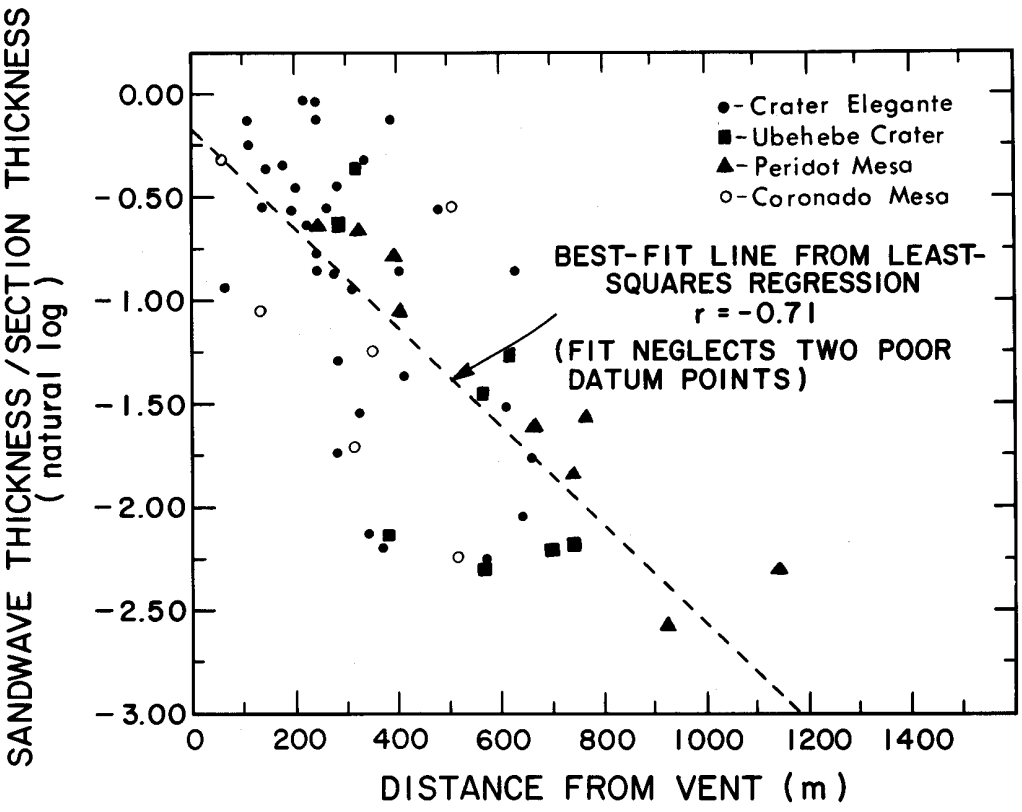

Figure 4. Plot of sandwave thickness (sandwave proportion) versus distance.

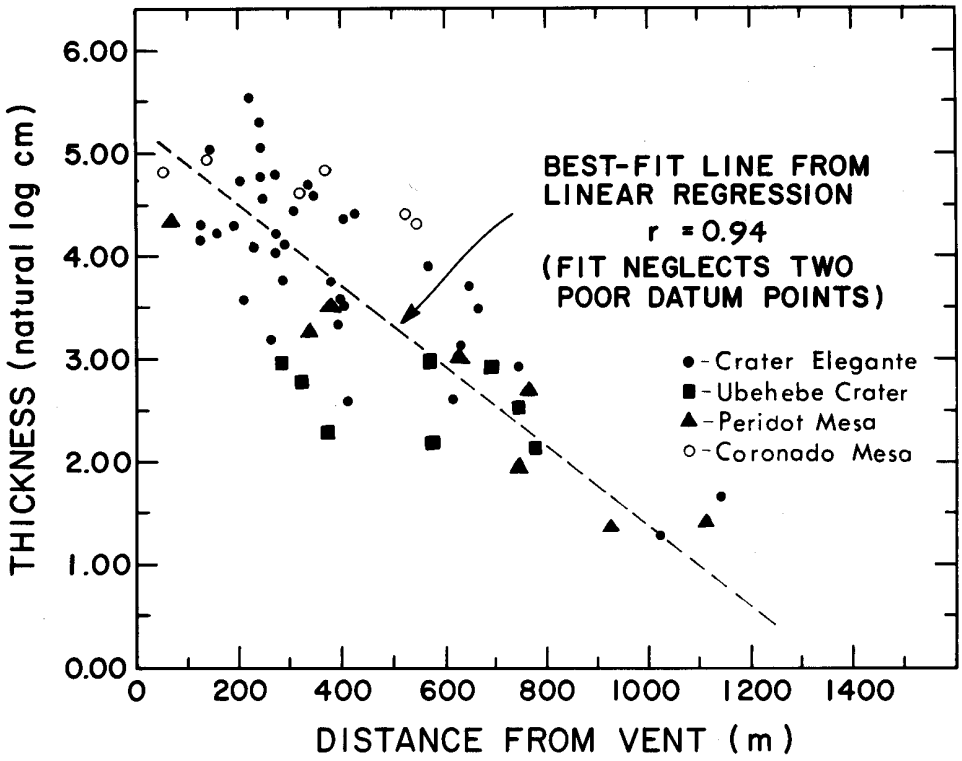

Figure 5. Plot of the average thickness of sandwave bedding sets versus distance.

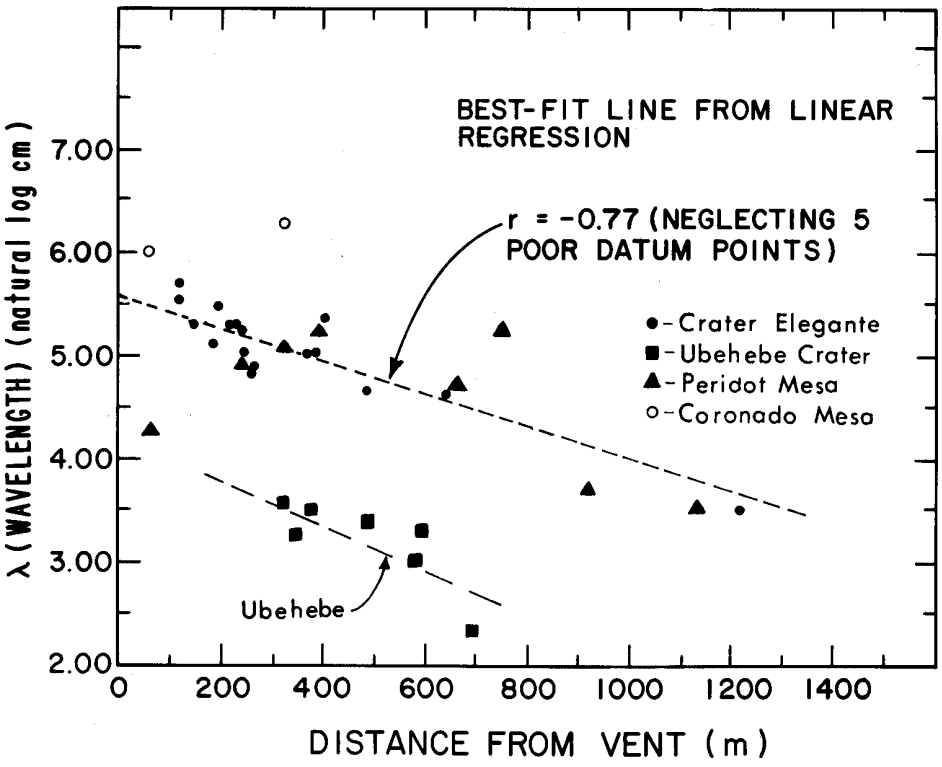

Figure 6. Plot of sandwave wave length versus distance.

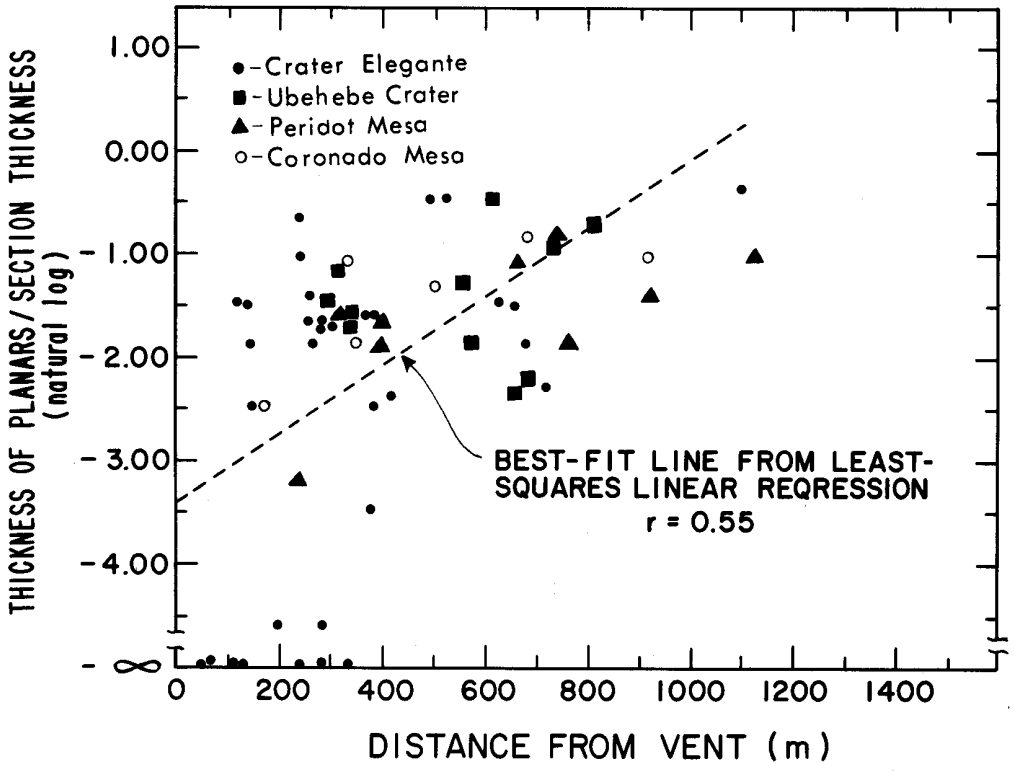

Figure 7. Plot of the ratio of planar bed thickness to section thickness (planar proportion) versus distance.

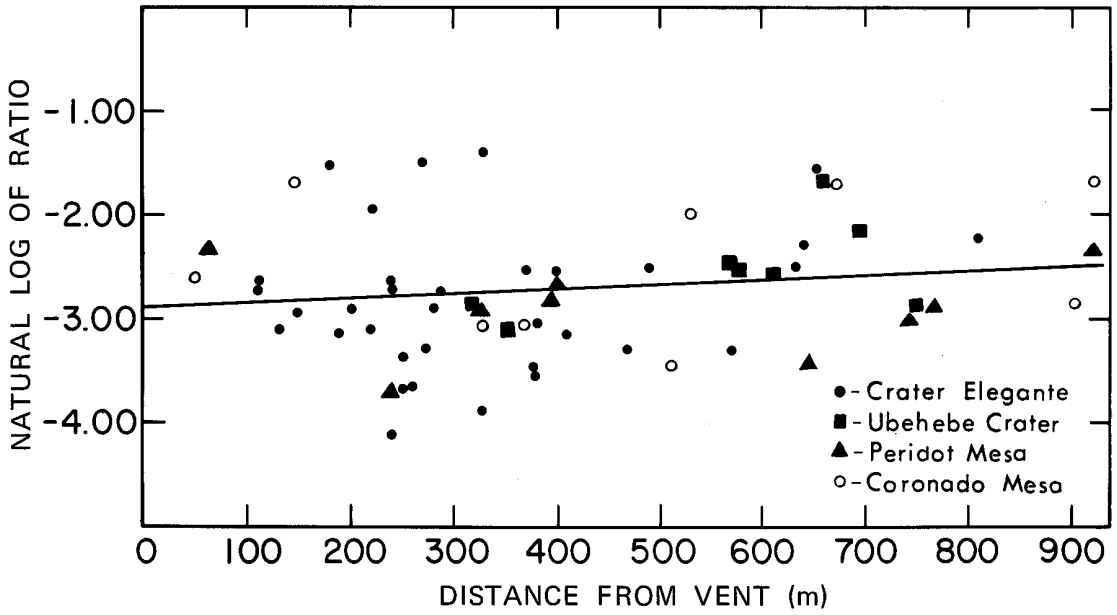

Figure 8. Plot of the ratio of massive bed thickness versus distance.

measured on eight sections, as well as a probable vent breccia, indicate a likely source. The tuff ring has an apparent diameter of 500 m, and surge deposits extend beyond 1,100 m from the vent. Sandwave beds dominate in the tuff ring and planar beds near the terminus of the surge deposit.

Ubehebe Crater. In northern Death Valley, California, Ubehebe Crater is a basaltic maar with a crater diameter of 800 m and a depth of 235 m. Its history and surge deposits with antidune structures were described by Crowe and Fisher (1973). The surge deposits are 50 m thick at the rim and extend for a distance of 820 m.

The surge deposits are extensively gullied and interbedded with pyroclastic-fall lapilli on the east and southeast sides of the crater where 12 sections were measured. At the crater rim, the surge deposits are best described as an explosion breccia of dominantly massive beds of large angular blocks and fewer sandwave beds of coarse sand and angular cobbles. Sorting improves away from the vent. Massive beds dominate in sections deposited along paleochannels. At distances of more than 700 m from the crater rim, sandwave beds are scarce or nonexistent.

Bishop Tuff. Pyroclastic surge deposits are interbedded with the upper part of Bishop Tuff air-fall tephra in eastern California. Sheridan (1965) and Bateman (1965) noted zones of finely bedded and inversely graded tephra associated with carbonized stringers within the air fall. Such surge deposits near the base of an ash-flow sheet previously have been described as "ground surge" by Sparks and Walker (1973). Finely bedded, crystal-rich zones within the ash-flow sheet, mapped as "sandy partings" by Crowder and Sheridan (1972), also appear to be of pyroclastic-surge origin. The 0.71-m.y.-old Bishop Tuff erupted from ring fractures around Long Valley caldera (Bailey and others, 1976). The surge associated with the Bishop Tuff air-fall tephra was erupted during the more energetic, initial phases of eruption that preceded the more continuous extrusion of ash flows. The surges may have resulted when the initial Plinian eruption column became unstable and started to choke. Only three sections at the base of the Bishop Tuff were found adequate for study, none of them closer than about 5 km from the likely vent area.

RESULTS

A three by three matrix of transition probabilities is constructed for each measured section. Each element in this matrix represents the number of a specific transition (say from a sandwave bed to a massive bed) divided by the total number of transitions measured for that section. These matrices are easily tested for a Markov property using a chi-square test (Davis, 1973). The transition-probability matrices used in this study are by definition transition-proportion matrices that facilitate visual assessment of the stratigraphic nature of the section they represent. Results indicate that surge sections show a high degree of a Markovian property, hence the sequence of bed forms in a section is the result of a nonrandom process.

The transition-probability matrix for each measured section can be characterized as most closely resembling one of three general matrix types that are distinguished by either (1) high probabilities (0.40 or greater) of S-S (sandwave to sandwave) transitions, M-M transitions moderate (0.11 to 0.39), and other transitions low (0.10 or less); (2) high or moderate probabilities of M-M transitions, S-S and P-P transitions moderate, and other transitions low; or (3) high or moderate probabilities of P-P transitions, M-M transitions moderate, and others low. These three general matrix types, picked to best represent

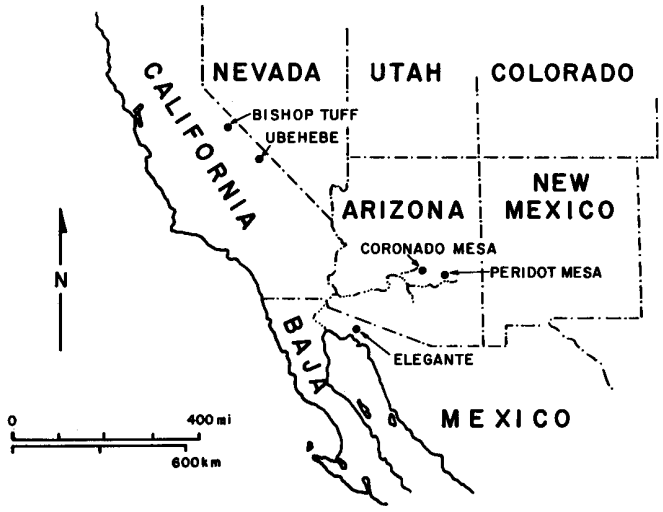

Figure 9. Location map of the five studied localities.

the range of observed matrices, define sections of the sandwave, massive, and planar types, respectively. Each section is classified by a least-squares comparison of its transition-probability matrix with the three general transition-probability matrices given below.

SANDWAVE	MASSIVE	PLANAR
0.48 0.10 0.02	0.20 0.05 0.03	0.10 0.02 0.02
0.10 0.20 0.02	0.05 0.45 0.03	0.02 0.20 0.06
0.02 0.02 0.04	0.03 0.03 0.12	0.02 0.06 0.50

Pyroclastic-Surge Facies

Three facies of pyroclastic surge are defined according to a Markov characterization of stratigraphic sections. In the sandwave facies, sandwave and massive beds are the dominant bed form deposited; in the massive facies, massive, sandwave, and planar beds are all significant; and in the planar facies, planar and massive beds are the dominant bed form deposited.

A computer program was written to construct and characterize the transition-probability matrix for each section and to generate hypothetical graphic sections from their matrices (Fig. 10). The computer graphic sections provide a means to check the validity of the numerical data by direct comparison with sketches of the actual sections.

Lateral variation of bed-form types is shown by composite sections for selected distance intervals away from the vent. The intervals are roughly one-third of the radius of the surge deposits giving (1) sections proximal to the vent, (2) sections at intermediate distances from the vent, and (3) sections at distal portions of the deposit. A composite section is obtained by averaging the transition-probability matrices of all the sections within an interval. The resulting composite matrix can be characterized as to facies type by a least-squares comparison with the three general matrices, as was done with individual sections. Composite sections at each locality show the same trend, except for the Bishop Tuff where no sections near the vent were found. Proximal sections are a sandwave type, sections of an intermediate-distance interval are a massive type, and distal sections are a planar type.

Facies maps show the extent of sections having the same Markov characterization. Facies maps for the five localities (Figs. 11 through 15) further document the lateral variation described by the composite stratigraphic sections. A sandwave facies directly surrounds the vent, a massive facies is at intermediate distances, and a planar facies encircles the vent at distal portions of the deposit. For each locality, deviation of facies contacts from a perfect concentric pattern is dependent on sample density, degree of preservation, topographic effects on the surge cloud, variations of vent location during the eruption, transport direction of surge cloud, and energy of the surge. At Crater Elegante and Ubehebe Crater, gullies funneled the surge clouds, producing marked protuberances in facies contacts. At Peridot Mesa, thickening of the capping basalt flow suggests that a pre-eruption valley extended from the vent toward the northeast. Surge-facies contacts also could be inflected in that direction, as suggested by the map. Although an adequate number of sections was not measured for the Bishop Tuff, a similar facies pattern may be inferred from existing information and paleotopography.

A vertical facies variation also exists at Crater Elegante. The deposit may be subdivided into three stratigraphic zones, each corresponding to an eruptive phase (Gutmann, 1976, oral commun.). Each zone has its own distinct facies distribution determined in part by the energy of activity and changes in size of the vent. The facies suggest an initial high energy phase, a middle slackening of eruptive energy, and a final violent phase.

DISCUSSION AND CONCLUSIONS

Eruptions that produce pyroclastic surges involve release of large volumes of steam or carbon dioxide capable of fluidizing some of the particles carried by surges. Fluidization has been proposed as a process of pyroclastic emplacement by many authors since Reynolds' (1954) paper. McTaggart (1960) and Brown (1962) discussed trapped gases and exsolving gases as lubricants to explain the mobility of nuées ardentes. Nakamura (1966) described a turbulent, fluidized cloud moving close to the ground as a result of the phreatomagmatic eruptions of Taal volcano in 1965. Ollier (1967) discussed fluidization in maar volcanism, as have subsequent authors. Pai and others (1972) developed a model that suggests that ash-flow particles are fluidized, and Schleicher (1974) followed by Sparks (1976) further expanded the idea. Sheridan and Updike (1975) explained various bed forms in a pyroclastic-surge (base-surge) deposit by fluidized transport of tephra.

Industrial particulate matter is fluidized by passing a fluid upward through a loose bed. When the pressure drop per unit area throughout the bed becomes greater than the weight of the bed, the system is fluidized and in ideal cases acts as a Newtonian fluid. Detailed descriptions of the engineering aspects of fluidization are covered in Leva (1959) and Kunii and Levenspiel (1969).

The application of the principles of fluidization to pyroclas-

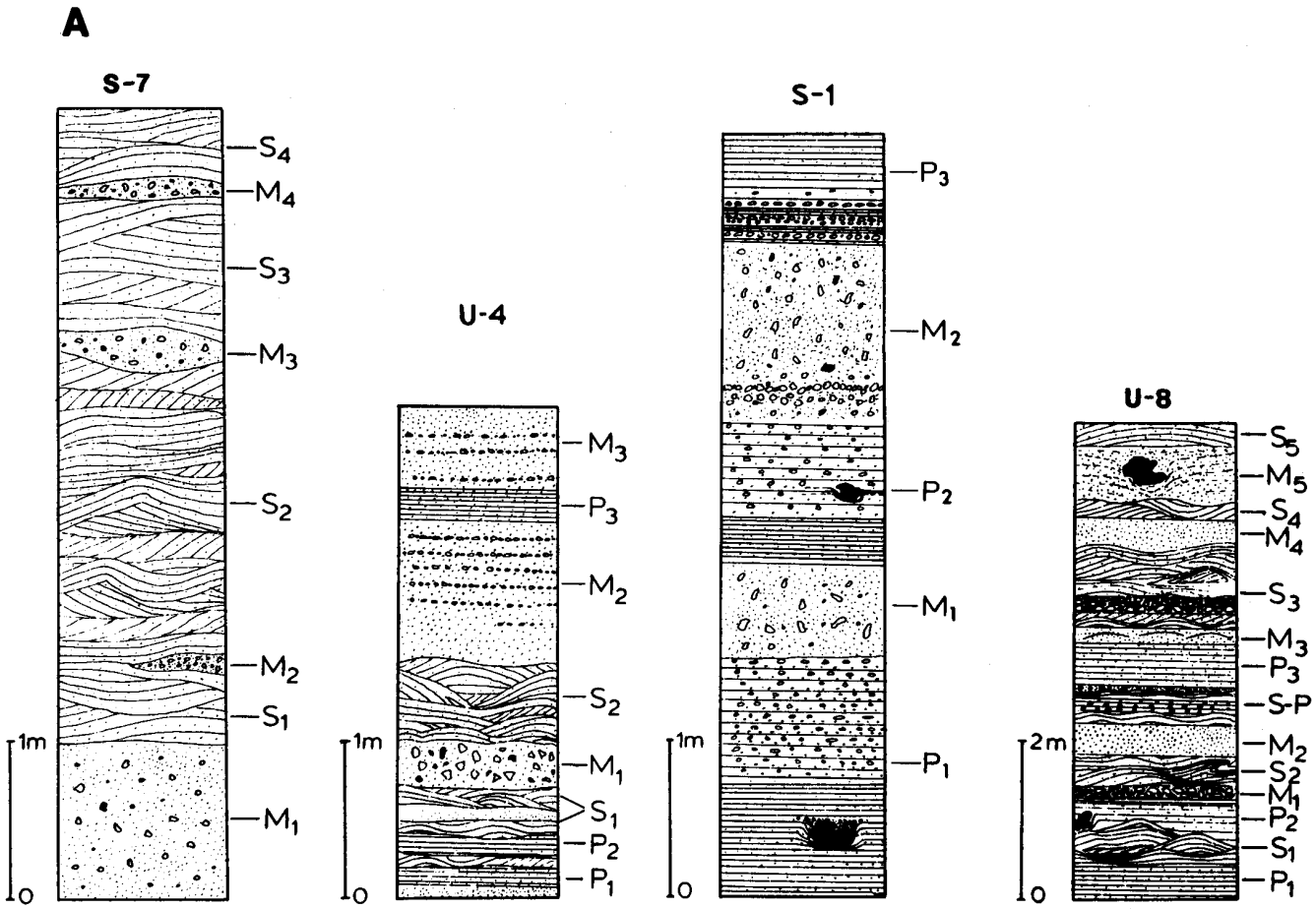

Figure 10 (facing pages). Results of the Markov analysis of four example surge sections. S-1 and S-7 are from Coronado Mesa, U-4 and U-8 from Ubehebe Crater. (A) Sketches of the four examples of measured sections where bed forms are denoted "S" for sandwave beds, "M" for massive beds, and "P" for planar beds. (B) Printout from the computer program showing the section characterization, transition probability, the general (theoretical) matrix of closest comparison, and the hypothetical graphic section generated for the section. For the computer graphic section, "----" denotes a planar bed, "O . .-. . O" a massive bed, and "SSSS" a sandwave bed.

tic-surge transport requires a careful examination of surge conditions and a precise definition of the mechanisms involved. The eruptive surge explosion inflates a cloud of particles dispersed in a matrix fluid of hot volatiles. As the cloud races outward from the vent, the paths followed by particles are effected by a number of rapidly changing parameters: upward gas velocity, local particle concentration, and radial surge velocity. As gas is lost from the system, particle fraction shows a progressive increase with time. In the strict sense, fluidization applies only to those parts of the system where the vertical pressure drop balances the mass concentration.

The progressive concentration of particles in the surge produces a pressure gradient by confining the interstitial fluid, but the upward velocity of gases is generally insufficient to fluidize the system. This process is similar to liquifaction in subaqueous systems (Lowe, 1976). Gas pressure, however, greatly reduces internal friction, causing an increase in the mobility of the surge. The origin of this internal pressure is twofold: (1) initial collapse of the surge cloud because of particle settling and (2) conversion of potential energy to kinetic energy as the cloud moves downslope from the vent.

Surge clouds are not strictly fluidized, but may more closely approximate a gas leakage model as Shreve (1968) suggested for gravity avalanches. In fluidized beds, bulk system parameters such as upward gas velocity, void fraction, and thickness of the flowing bed remain more or less uniform with time. For pyroclastic surges the same parameters rapidly decrease with time due to bulk subsidence. For this reason the surge system might better be termed one of deflation, following the use of Sheridan and Ragan (1976). This emphasizes the mechanism that provides mobility to the system. The basic parameters of fluidization, however, still apply.

Fluidized (deflating) systems can be subdivided into three regimes: (1) fixed to incipiently fluidized beds, (2) dense-phase fluidized beds, and (3) lean-phase fluidized beds. For rhyolitic tephra of moderate to poor sorting, an incipiently fluidized bed would have a void fraction (Φ) of approximately 0.4 to 0.6, corresponding to a bulk density of 1.2 to 1.0. Leva (1959) defined the dense-phase fluidized regime as having a solid fraction (G) of 0.1 to 0.4 (Φ = 0.9 to 0.6) and the lean-phase

B

SECTION S-7

SANDWAVE FACIES
DISTANCE FROM THE VENT 55.00 METERS
DEVIATION IN PROBABILITY
FROM THEORETICAL SECTION 0.05

TRANSITION PROBABILITY MATRIX				THEORETICAL PROBABILITY MATRIX		
	S	M	P	S	M	P
S	.72	.07	.00	.46	.10	.02
M	.09	.13	.00	.10	.20	.02
P	.00	.00	.00	.02	.02	.04

SECTION U-4

MASSIVE FACIES
DISTANCE FROM THE VENT 575.00 METERS
DEVIATION IN PROBABILITY
FROM THEORETICAL SECTION 0.01

TRANSITION PROBABILITY MATRIX				THEORETICAL PROBABILITY MATRIX		
	S	M	P	S	M	P
S	.20	.06	.02	.20	.05	.03
M	.04	.48	.04	.05	.45	.04
P	.04	.02	.11	.03	.03	.11

SECTION S-1

PLANAR FACIES
DISTANCE FROM THE VENT 925.00 METERS
DEVIATION IN PROBABILITY
FROM THEORETICAL SECTION 0.04

TRANSITION PROBABILITY MATRIX				THEORETICAL PROBABILITY MATRIX		
	S	M	P	S	M	P
S	.00	.00	.00	.10	.02	.02
M	.00	.29	.10	.02	.20	.06
P	.00	.08	.54	.02	.06	.50

SECTION U-8

SANDWAVE FACIES
DISTANCE FROM THE VENT 320.00 METERS
DEVIATION IN PROBABILITY
FROM THEORETICAL SECTION 0.05

TRANSITION PROBABILITY MATRIX				THEORETICAL PROBABILITY MATRIX		
	S	M	P	S	M	P
S	.31	.05	.04	.40	.10	.02
M	.09	.18	.02	.10	.28	.02
P	.04	.04	.24	.02	.02	.04

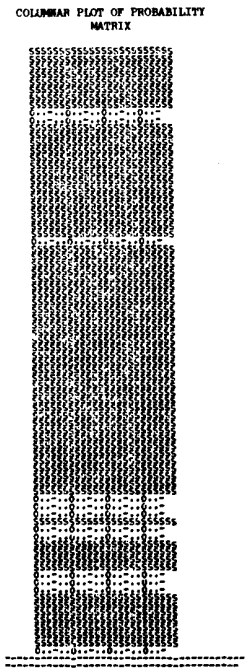

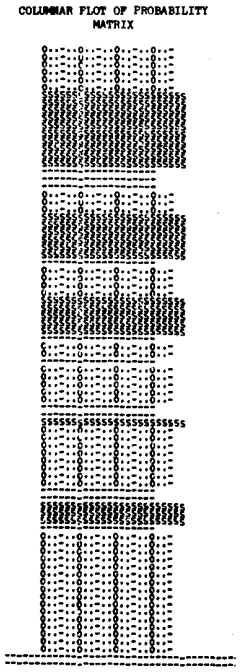

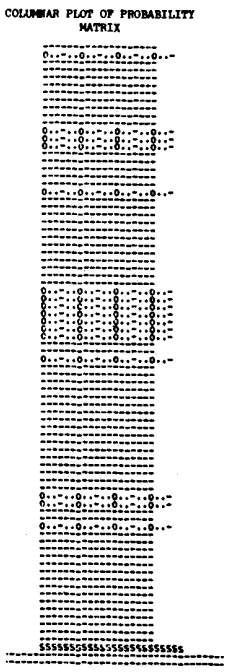

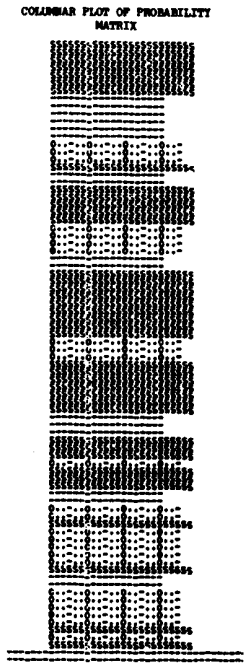

as having a solid fraction of less than 0.1 ($\Phi > 0.9$). The void fraction is an important concept in the flow of particles in deflating systems, because it critically influences the development of textures (Bagnold, 1941, 1954; Sanders, 1965; Carter, 1975).

Clot slugging or choking (Kunii and Levenspiel, 1969) of fluidized systems may influence surge formation. Clots of particles with a greater bulk density than the surrounding region may fall back through a fluidized eruptive column above a vent to choke or block the flow of gas. Subsequently they are blown clear in a "sudden surge" (Lewis and others, 1949). Choking could initiate surges within the vent.

Three primary types of bed forms have been described in surge deposits: sandwave beds that are deposited from a viscous flow (Bagnold, 1941); planar beds that are deposited from an inertial flow (Bagnold, 1954); and massive beds that are deposited from interaction of viscous and inertial flow. Application of these flow systems to surge flow follows.

The three rectangles of Figure 16 represent cross sections of cylinders filled with equidimensional spheres. The rectangular sections pass through planes of hexagonal closest packing. Three different void fractions are illustrated: (A) incipient fluidization, (B) dense-phase fluidized, and (C) lean-phase fluidized. In case A ($\Phi = 0.6$), the closeness of neighboring particles is apparent. During lateral transport of these particles over a surface, momentum is transfered by particle collisions. The fluid viscosity of the interstitial gas has a minor effect compared to the dispersive pressure of grain interactions, which is related to the applied shear stress, particle diameter, density, and surface roughness. Flow of this nature is called "inertial" (Bagnold, 1954) and is within the laminar flow regime. In case C ($\Phi = 0.95$), the particles are sufficiently spaced so that during flow, the system acts as a viscous Newtonian fluid with negligible net dispersive pressure from collisions, provided the distribution of grains remains isotropic. Flow of this nature is called "viscous" and has Reynolds numbers within the turbulent flow regime (Bagnold, 1941, 1954). Finally, in case B ($\Phi = 0.75$), both dispersive forces (inertial) and viscous forces are significant. This results in a transitional situation between viscous and inertial flow that for air-steam-sand

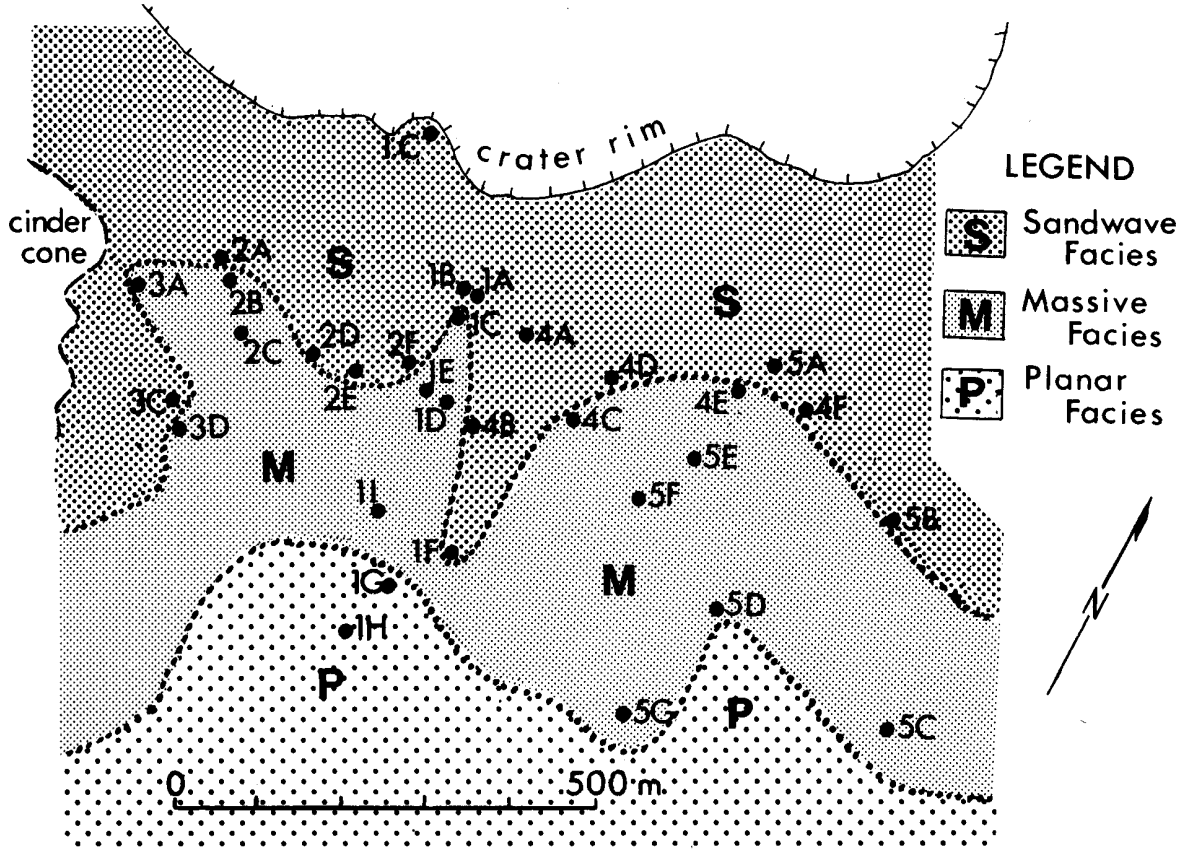

Figure 11. Pyroclastic-surge facies map of the south side of Crater Elegante.

mixtures is likely to be turbulent. Viscous and inertial (grain flow) transport have been discussed in great detail by Bagnold (1954) and have been applied to subaqueous flows by Carter (1975). The void fraction (degree of inflation) is probably the most important factor in determining particle transport in a surge, but flow velocity, grain-size distribution, surface roughness, flow density, and cohesion are also important.

Development of Bed Forms

Planar Beds. Planar beds are almost invariably inversely graded, which precludes an origin by normal gravity fallout from a turbulent flow regime. Laminar grain-flow is the likely transport mechanism. Because inverse grading exists in individual beds, each bed is likely to result from a zone of inertial flow within a surge.

Bagnold (1954) described a process by which inverse grading results from inertial flow. Individual grains seek positions of lowest energy or shear stress. Since the grain-dispersive pressure increases as the square of the grain diameter, large grains, being subjected to more collisions than small grains, will seek lower shear-stress regimes. Larger grains move to free surfaces or upper parts of beds where lower shear stress exists, and inverse grading results. The void fraction in a surge flow that deposits planar beds is between 0.5 (at rest) and 0.6 (lower limit of fluidization).

Sandwave Beds. Sheridan and Updike (1975) argued for deposition of sandwave beds from a lean-phase fluidized flow in which saltation of particles occurs, analogous to eolian desert dunes (Bagnold, 1954). For grains to saltate freely over a surface, a relatively small concentration ($\Phi > 0.9$) of particles assures undisturbed trajectories for individual particles. Variations in textures, as well as in size distribution in sandwaves, may be controlled by fluctuation of flow velocity, the source size-distribution, and surface cohesion and roughness.

Massive Beds. Grain-size characteristics together with stratigraphic position and textures of massive beds appear to be the result of a transport mode intermediate to those that produce planar and sandwave beds. Grain-size distributions of massive beds are polymodal (Sheridan and Updike, 1975), apparently a combination of the grain-size distributions of planar and sandwave beds. Massive beds usually occur stratigraphically between planar and sandwave beds and grade into both. In an intermediate transport mode where both inertial and viscous forces are significant, the system would be densely fluidized ($\Phi = 0.6$ to 0.9). Such a flow regime would be turbulent, but neither inertial, grain-dispersive effects, nor viscous effects would dominate.

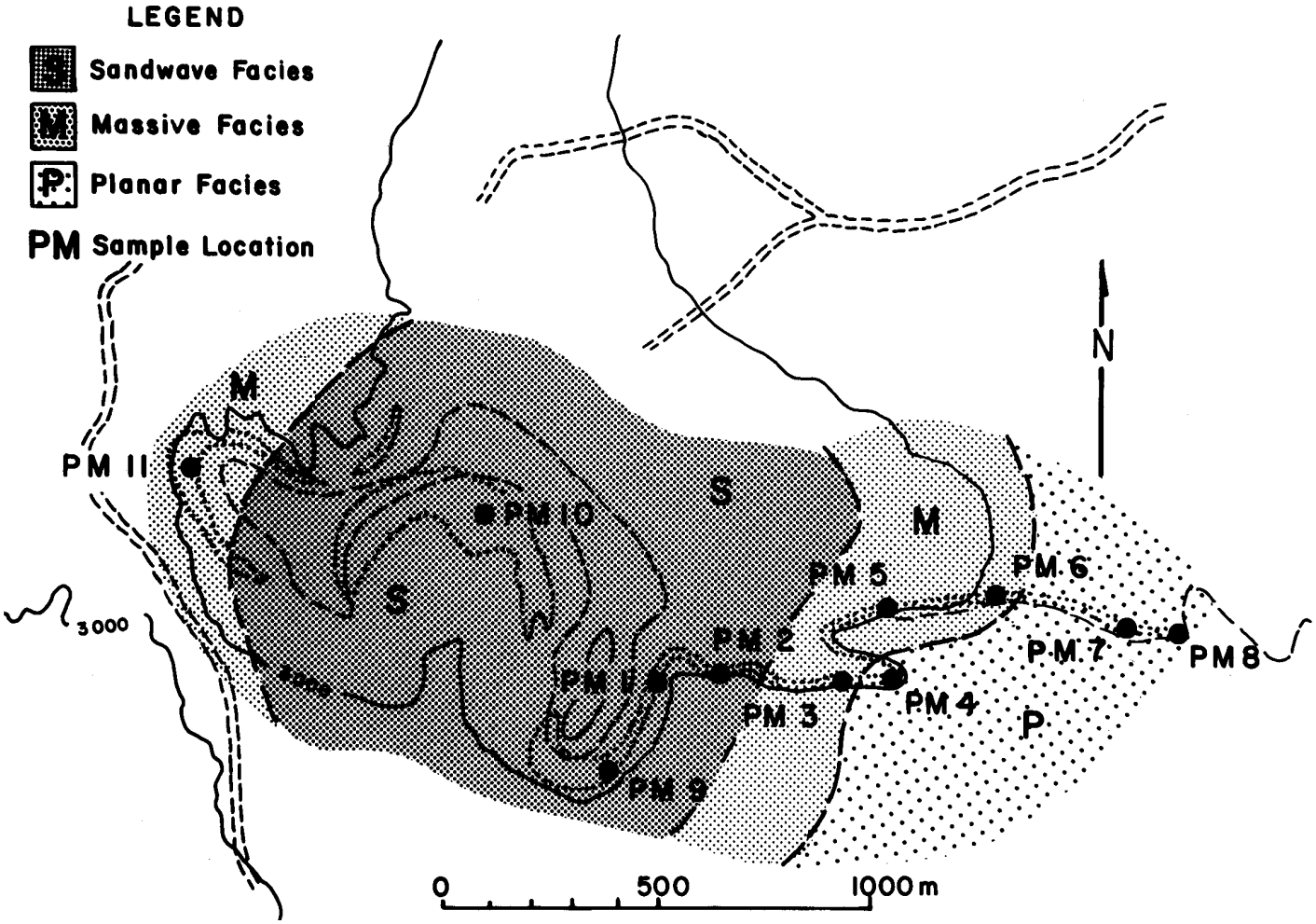

Figure 12. Pyroclastic-surge facies map of Peridot Mesa. The vent area is near PM-10, and the dotted lines surround present surge deposit exposures.

Reconstruction of the Surge Cloud

The composite columnar sections for the three distance intervals that have been calculated earlier may be used to characterize the deposits left by all the surges that have passed the area. By assuming appropriate inflation for the three basic bed forms, a composite surge cloud can be constructed for each distance interval. Such a reconstructed cloud represents an expanded section, assuming that the solid fraction generally decreases upward, as in industrial systems. Figure 17 shows reconstructed surge clouds for the three distance intervals of each locality. At any distance interval, the deposit is composed of many surge beds, representing a spectrum of flow densities that can be time modeled by the Markov matrix. The reconstructed surge clouds are an integration of the complete series of surges responsible for the deposits at any one point. As the cloud passes each interval, its height decreases. The proportion of lean- to dense-phase fluidized regimes decreases as does the proportion of dense-phase to incipiently fluidized regimes. The exceptions in the displayed figures are likely to have been caused by topographic and sampling effects upon the input data. These plots are strong support for the deflation of individual surge clouds as they move away from the vent.

A Model of Pyroclastic Surge: Its Fluidization and Deflation

A sequential model can explain lateral facies variations in surge deposits away from a vent.

1. On eruption, a pyroclastic surge is greatly inflated (fluidized) by one or more of the following mechanisms: (a) entrapped phreatomagmatic steam, (b) rapid exsolution of magmatic volatiles, and (c) bulk subsidence by gravitational column collapse (Sparks and Wilson, 1976).

2. The greatly inflated cloud travels horizontally or down gentle slopes away from the vent due to gravity and/or the

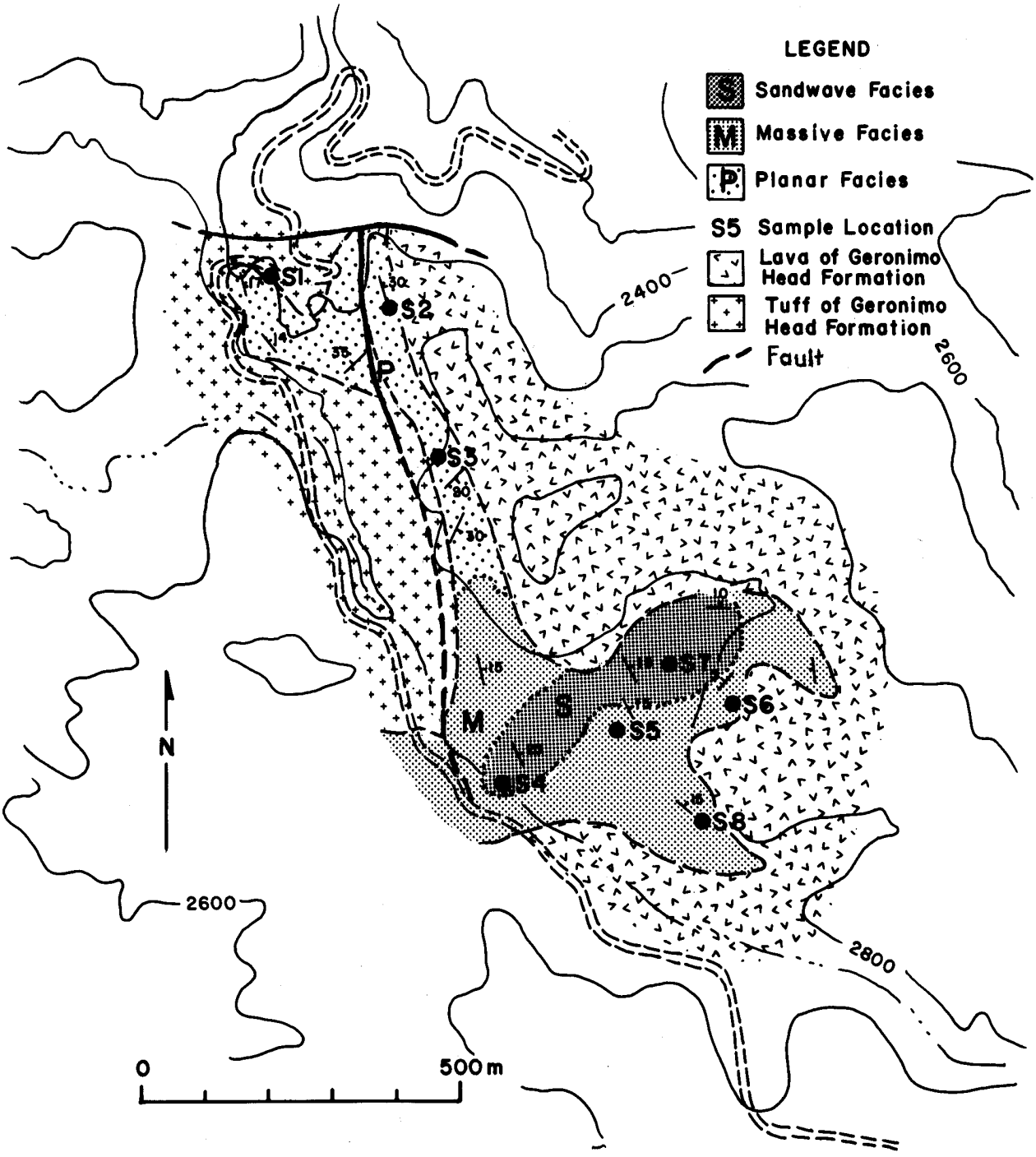

Figure 13. Pyroclastic-surge facies map of Coronado Mesa. The apparent vent area is near S-7.

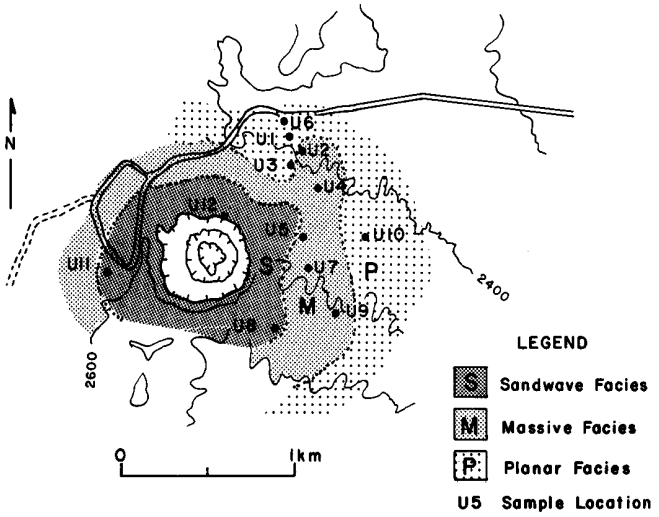

Figure 14. Pyroclastic-surge facies map of Ubehebe Crater.

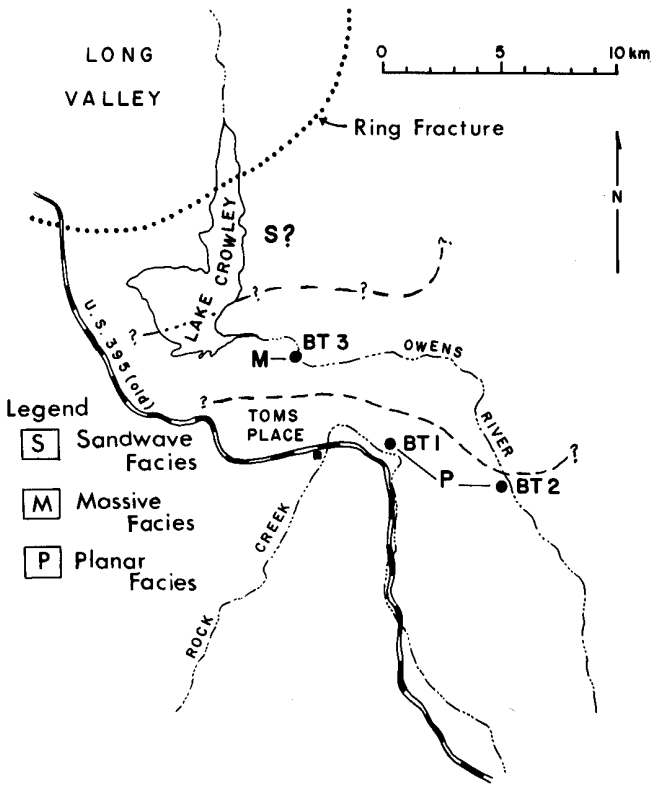

Figure 15. Pyroclastic-surge facies map of the Bishop Tuff.

horizontal velocity component of fluidized particles within the cloud.

3. Near the vent, the cloud is dominantly a lean-phase fluidized system resulting in viscous flow. Grains are transported and deposited in a saltation mode forming sandwave beds. Clots of densely fluidized material may also deposit lenses of massive beds.

4. As the cloud continues to move away from the vent and gas escapes, the cloud deflates until different parts are lean-phase fluidized, densely fluidized, and nonfluidized. Here transport is divided into regimes of viscous, inertial-viscous, and inertial flow. Resulting beds are massive, interfingered with sandwave and planar beds.

5. As the surge moves farther from the vent, most entrapped fluidizing gas escapes. Surges are nonfluidized, but possible zones of dense fluidization may persist in the cloud. Inertial flow dominates, producing inversely graded planar beds and some massive beds from densely fluidized zones. At this point, the flow is quickly halted by drag of sliding friction.

In the resulting deposit, sandwave and massive beds dominate near the vent (sandwave facies); interbedded planar, massive, and sandwave beds dominate at intermediate distances (massive facies); and planar and massive beds dominate at distal parts of the deposit (planar facies). The schematic diagram in Figure 18 illustrates a surge cloud as it moves away from the vent, showing its deflation-defluidization and zones of different transport modes.

Complications of the Model. Three basic complications affect the model: (1) Any section records the superposition of many surges erupted during a sequence of volcanic explosions at one vent. Each surge is of different size and energy, and transports tephra of varying characteristics. (2) Topographic and meteorologic parameters may effect the surge cloud and its deposits. (3) Particles of various sizes and densities in a flow require different residence times to come into equilibrium with their distinct modes of transport and deposition.

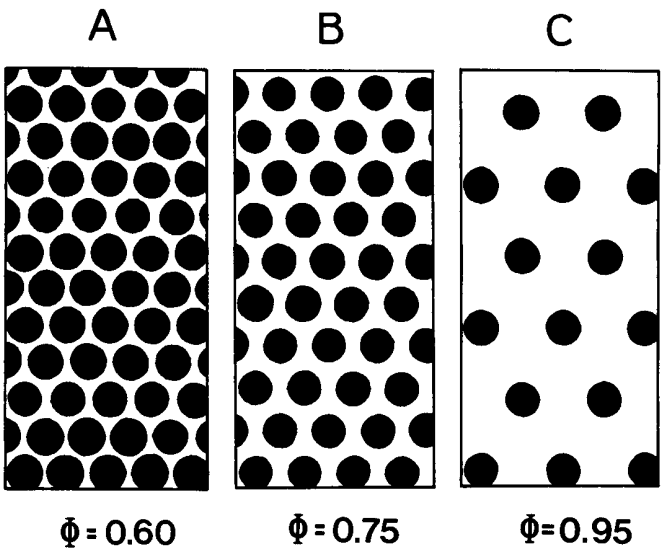

Figure 16. Representation of cross sections of cylinders filled with equidimensional spheres. (A) Spacing of particles at the incipient fluidization level (void fraction, $\Phi = 0.60$). (B) Spacing of particles at a dense-phase fluidization level ($\Phi = 0.75$). (C) Spacing of particles at a lean-phase fluidization level ($\Phi = 0.95$).

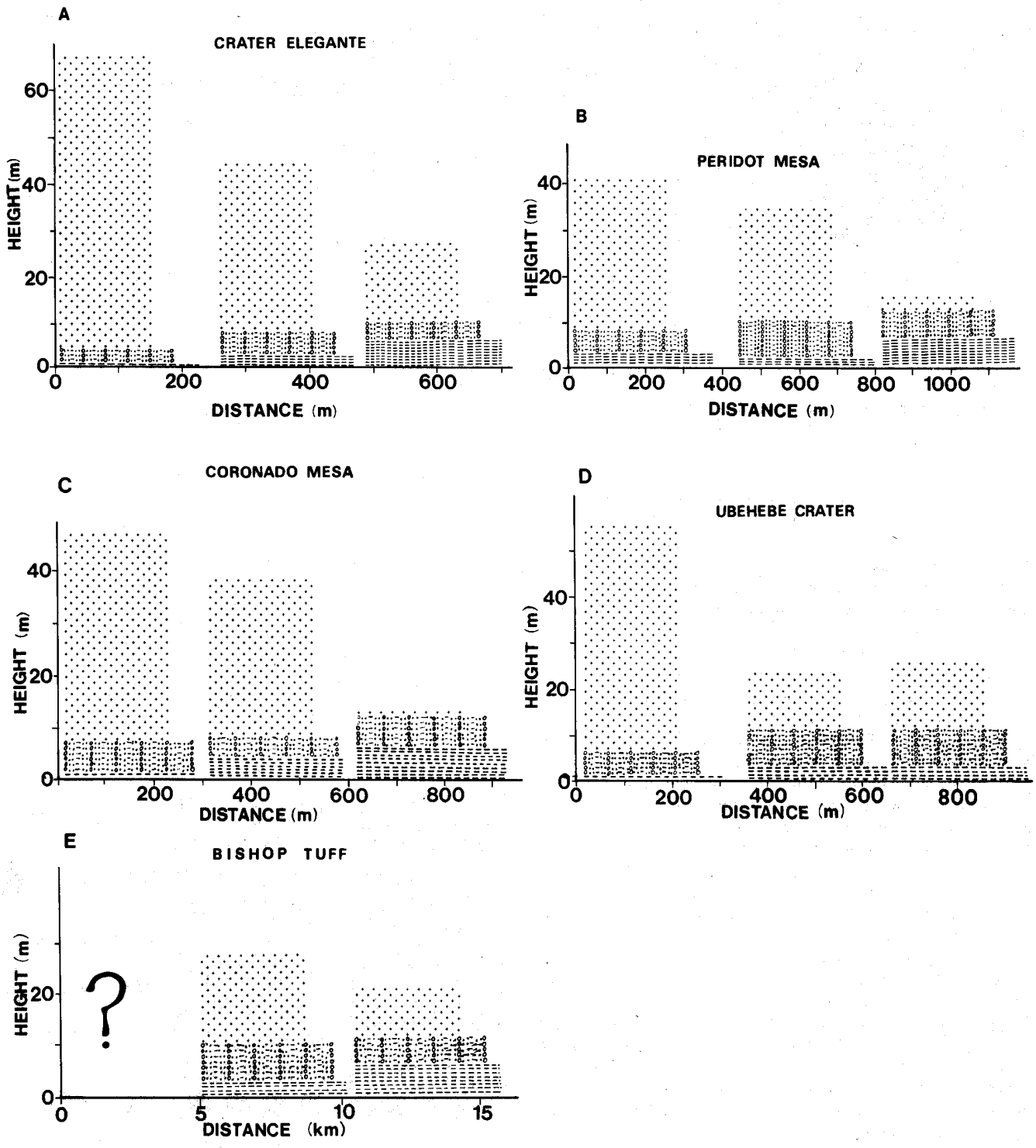

Figure 17. Reconstructions of "average" surge clouds passing three distance intervals at the localities studied. Symbols are "+ + + +" for the lean-phase fluidized region of the cloud, "O . .-. . O" for the dense-phase, and "----" for the nonfluidized region of the cloud. Note the apparent deflation of the cloud with increasing distance traveled from the vent.

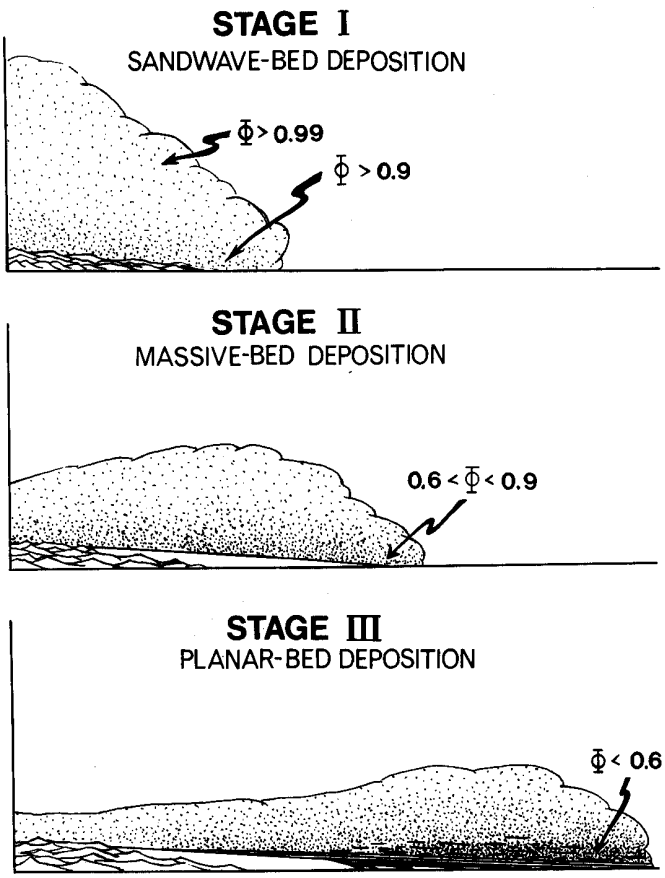

Figure 18. Diagrammatic illustration of a surge cloud at three stages of its development: Stage I near the vent, Stage II at intermediate distances from the vent, and Stage III near the terminus of its flow. During Stage I, flow is highly inflated ($\Phi > 0.9$), and deposition of sandwave beds results. At Stage II the cloud has deflated ($0.6 < \Phi < 0.9$), with massive bed deposition resulting. Finally, at Stage III, the cloud has deflated until it is an avalanching-type flow ($0.5 < \Phi < 0.6$), planar beds are deposited, and the flow stops.

ACKNOWLEDGMENTS

We thank Grant Heiken, Wolfgang Elston, Charles Chapin, and David Krinsley for their helpful reviews. Illustrations were done in part by Luween Smith of the Los Alamos Scientific Laboratory and Sue Selkirk of Arizona State University. Bruce Crowe offered many helpful suggestions.

REFERENCES CITED

Bagnold, R. A., 1941, The physics of blown sand and desert dunes: London, Methuen and Co., 265 p. (reprinted 1954).

——1954, Experiments on a gravity-free dispersion of large-solid spheres in a Newtonian fluid under shear: Royal Society of London Proceedings, v. 225, p. 29–63.

Bailey, R. A., Dalrymple, G. B., and Lanphere, M. A., 1976, Volcanism structure, and geochronology of Long Valley caldera, Mono County, California: Journal of Geophysical Research, v. 81, p. 725–744.

Bateman, P. C., 1965, Geology and tungsten mineralization of the Bishop district, California: U.S. Geological Survey Professional Paper 470, 208 p.

Brown, M. C., 1962, Nuees ardentes and fluidization: A discussion, together with reply by K. C. McTaggart: American Journal of Science, v. 260, p. 467–476.

Carter, R. M., 1975, A discussion and classification of subaqueous mass transport with particular application to grain-flow, slurry-flow, and fluxoturbidites: Earth-Science Reviews, v. 11, p. 145–177.

Crowder, D. F., and Sheridan, M. F., 1972, Geologic map of the White Mountain Peak quadrangle, Mono County, California: U.S. Geological Survey Map GQ-1012.

Crowe, B. M., and Fisher, R. V., 1973, Sedimentary structures in base-surge deposits with special reference to cross-bedding, Ubehebe Craters, Death Valley, California: Geological Society of America Bulletin, v, 84, p. 663–682.

Davis, John C., 1973, Statistics and data analysis in geology: New York, John Wiley & Sons, Inc., 550 p.

Fisher, R. V., 1966, Mechanism of deposition from pyroclastic flows: American Journal of Science, v. 264, p. 350–363.

——1976, The mobility of hot pyroclastic flows: Geological Society of America Abstracts with Programs, v. 8, no. 5, p. 586.

Fisher, R. V., and Waters, A. C., 1969, Bedforms in base-surge deposits: Lunar implications: Science, v. 165, p. 1349–1352.

——1970, Base surge bedforms in maar volcanoes: American Journal of Science, v. 268, p. 157–180.

Gault, D. E., 1973, Displaced mass, depth, diameter, and effects of trajectories for impact craters formed in dense crystalline rocks: The Moon, v. 6, p. 32–44.

Gutmann, J. T., 1976, Geology of Crater Elegante, Sonora, Mexico: Geological Society of America Bulletin, v. 87, p. 1718–1729.

Harbaugh, J. W., and Bonham-Carter, C. G., 1970, Computer simulation in geology: New York, John Wiley & Sons, Inc., 575 p.

Inman, D. L., 1952, Measures for describing the size distribution of sediments: Journal of Sedimentary Petrology, v. 22, p. 125–145.

Jahns, R. H., 1959, Collapse depressions of the Pinacate volcanic field, Sonora, Mexico: Arizona Geological Society, Southern Arizona Guidebook II, p. 165–184.

Kunii, D., and Levenspiel, O., 1969, Fluidization engineering: New York, John Wiley & Sons, Inc., 534 p.

Leva, M., 1959, Fluidization: New York, McGraw-Hill Book Co., 327 p.

Lewis, W. K., Gilliland, E. R., and Bauer, W. C., 1949, Characteristics of fluidized particles: Industrial and Engineering Chemistry, v. 41, no. 6, p. 1104–1124.

Lowe, D. R., 1976, Subaqueous liquified and fluidized sediment flows and their deposits: Sedimentology, v. 23, p. 285–308.

Masursky, H., 1968, Preliminary geologic interpretations of Lunar Orbiter photography, *in* 1969 NASA Authorization, Part 3, 337 p.

McTaggart, K. C., 1960, The mobility of nuees ardentes: American Journal of Science, v. 258, p. 369–382.

Moore, J. G., 1967, Base surge in recent volcanic eruptions: Bulletin Volcanologique, v. 30, p. 337–363.

Nakamura, K., 1966, The magmatophreatic eruptions of Taal Volcano in 1965, Philippines: Geology Magazine (Japan), v. 75, no.2 (751), p. 93–104 (in Japanese).

Ollier, C. D., 1967, Maars, their characteristics, varieties, and definition: Bulletin Volcanologique, v. 31, p. 45–73.

Pai, S. I., Hsieh, T., and O'Keefe, J. A., 1972, Lunar ash flow with

heat transfer, *in* Proceedings of the Third Lunar Science Conference, Supplement 3: Geochimica et Cosmochimica Acta, v. 3, p. 2689–2711.

Reynolds, A. F., 1954, Fluidization as a geological process, and its bearing on the problem of intrusive granites: American Journal of Science, v. 252, no.10, p. 577–613.

Richards, A. F., 1959, Geology of the Isla Revillagigedo, Mexico, 1. Birth and development of Volcan Barcena, Isla San Benedicta (1): Bulletin Volcanologique, ser. 2, v. 22, p. 73–123.

Sanders, J. E., 1965, Primary sedimentary structures formed by turbidity currents and related to resedimentation mechanisms, *in* Middleton, G. V., ed., Primary sedimentary structures and their hydrodynamic interpretation: Society of Economic Paleontologists and Mineralogists Special Publication 12, p. 192–219.

Schleicher, D., 1974, Emplacement mechanism of the Miraleste tuff bed Palos Verdes Hills, California: Geological Society of America Bulletin, v. 85, p. 505–512.

Schmincke, H. U., Fisher, R. V., and Waters, A. C., 1973, Antidune and chute and pool structures in the base surge deposits of the Laacher See area, Germany: Sedimentology, v. 20, p. 553–574.

Sheridan, M. F., 1965, The petrology of the Bishop Tuff [Ph.D. dissert.]: Stanford University, 142 p.

——1968, Volcanic geology along the western part of the Apache Trail, Arizona: Arizona Geological Society, Southern Arizona Guidebook III, p. 227–229.

——1971, Particle-size characteristics of pyroclastic tuffs: Journal of Geophysical Research, v. 76, p. 5627–5634.

——1976, Emplacement of ash-flow tuffs: Geological Society of America Abstracts with Progams, v. 8, no. 5, p. 628–629.

Sheridan, M. F., and Maisano, M. D., 1975, Flowage mechanism of the 1965 Taal and 1964 Surtsey pyroclastic deposits [abs.]: International Union of Geodesy and Geophysics, Proceedings XVI General Assembly, p. 102.

Sheridan, M. F., and Ragan, D. M., 1976, Compaction of ash-flow tuffs, *in* Chilingarian, G. V., and Wolf, K. H., eds., Compaction of coarse-grained sediments, Volume 2: Amsterdam, Elsevier Scientific Publishing Co., p. 677–707.

Sheridan, M. F., and Updike, R. G., 1975, Sugarloaf Mountain tephra—a Pleistocene rhyolitic deposit of base-surge origin: Geological Society of America Bulletin, v. 86, p. 571–581.

Shreve, R. L., 1968, Leakage and fluidization in air-layer lubricated avalanches: Geological Society of America Bulletin, v. 79, p. 653–658.

Simons, D. B., and Richardson, E. V., 1966, Resistance to flow in alluvial channels: U.S. Geological Survey Professional Paper 422-J, p. J1–J61.

Sparks, R.S.J., 1976, Grain size variations in ignimbrites and implications for the transport of pyroclastic flows: Sedimentology, v. 23, p. 147–188.

Sparks, R.S.J., and Walker, G.P.L., 1973, The ground surge deposits; A third type of pyroclastic rock: Nature Physical Science, v. 241, p. 62–64.

Sparks, R.S.J., and Wilson, L., 1976, A model for the formation of ignimbrites by gravitational column collapse: Journal of the Geological Society of London, v. 132, p. 441–451.

Sparks, R.S.J., Self, S., and Walker, G.P.L., 1973, Products of ignimbrite eruptions: Geology, v. 1, p. 115–118.

Stuckless, J. S., and Sheridan, M. F., 1971, Tertiary volcanic stratigraphy in the Goldfield and Superstition Mountains, Arizona: Geological Society of America Bulletin, v. 82, p. 3235–3240.

Suneson, N. H., and Sheridan, M. F., 1975, Geology of the northern portion of the Superstition-Superior volcanic field, Maricopa and Pinal Counties, Arizona: Geological Society of America Abstracts with Programs, v. 7, no. 7, p. 1287–1288.

Walker, G.P.L., 1971, Grain-size characteristics of pyroclastic deposits: Journal of Geology, v. 79, p. 696–714.

Waters, A. C., and Fisher, R. V., 1971, Base surges and their deposits: Capelinhos and Taal Volcanoes: Journal of Geophysical Research, v. 76, p. 5596–5614.

Wohletz, K. H., and Sheridan, M. F., 1976, A model for base-surge deposits: Geological Society of America Abstracts with Programs, v. 8, no. 5, p. 645–646.

MANUSCRIPT RECEIVED BY THE SOCIETY OCTOBER 9, 1978
MANUSCRIPT ACCEPTED FEBRUARY 28, 1979

Printed in U.S.A.